Arabian Journal of Geosciences (2021) 14: 37
https://doi.org/10.1007/s12517-020-06416-1

REVIEW PAPER

A comprehensive review of SAR image filtering techniques: systematic survey and future directions

Ranjith Kumar Painam[1] · Suchetha Manikandan[1]

Received: 7 January 2020 / Accepted: 25 December 2020 / Published online: 7 January 2021

Abstract

The synthetic aperture radar (SAR) is an active instrument used in various atmospheric conditions and can generate images with high resolution. SAR is a satellite imaging technology, working under all weather conditions throughout the day and night. It operates at microwave (or radar) frequencies. For a SAR image, speckle noise is a natural characteristic that corrupts the radiometric quality from the image and can affect the visualization and analysis. Speckle is usually modeled as a multiplicative noise that reduces SAR image quality. The suppression of the speckle is a pre-processing step. The speckle noise reduction process is known as despeckling. There are methods available to reduce speckle noise. This paper reviews various speckle reduction methods by highlighting their merits and demerits.

Keywords Synthetic aperture radar · Satellite imaging · Despeckling · Multiplicative noise

Introduction

Speckle noise is a multiplicative noise that gives a grainy outlook to the image. Speckle noise in a synthetic aperture radar (SAR) image is typically severe, causing difficulties in image interpretation. Coherent signal scattering in SAR data generally causes image speckles, which is one of the main drawbacks of the SAR image. Speckle noise occurs when the scattering returns from every resolution cell interfere constructively or destructively and consequently produce brighter or darker pixels. The speckle noise prevents an accurate interpretation of the image. As a result, speckle reduction is of great importance in SAR image processing. Choosing the best filtering approaches for a SAR image is not optimized yet. We need to analyze more methodologies for this purpose. The main issue in SAR image processing is the reduction of speckle noise. Many despeckling techniques have been proposed based on the multiplicative speckle noise model (Choi and Jeong 2020a, b; Murugesan et al. 2020).

Using platform movement, SAR systems are installed on mobile platforms over a wide area to obtain a larger synthetic antenna, improving the azimuth resolution. Speckle occurs in SAR images due to the coherent interferences of waves reflected from multiple elementary scatters, which reduces the quality of the SAR image (Das et al. 2013; Oikonomidis and Pavlides 2017). SAR works well in all weather conditions. It is a remote sensing tool and applied for target recognition, military and civilian fields, topographic mapping, and environmental monitoring (Rajamani and Krishnaveni 2014; Ezzine et al. 2018). To process the SAR images into different task classification, segmentation, and detection requires speckle reduction (Gromek and Castaldo 2013; Sun et al. 2017; Ahmed et al. 2018; Haldar et al. 2019; Mi et al. 2019). Due to the speckle appearing in SAR images, identifying the targets and analyzing different scenes are difficult (Mansourpour et al. 2006).

The anisotropic Gaussian kernel-minimum mean square error (AGK-MMSE) filter (D'hondt et al. 2006) is used for speckle reduction in the SAR image. Using this filter, the quality of the filtering is good. But the drawback is that the bias is weak for homogeneous areas and this filter uses a higher window size of 9 × 9. The mean shift filter (Jarabo-Amores et al. 2010) uses lower window sizes of 3 × 3 and 5 × 5 but the drawback of this filter is an issue with comparing the

Responsible Editor: Biswajeet Pradhan

✉ Suchetha Manikandan
suchetha.m@vit.ac.in

Ranjith Kumar Painam
ranjithkumar.painam2015@vit.ac.in

[1] School of Electronics Engineering, VIT University, Chennai, Tamil Nadu, India

images with different resolutions. The speckle reduction anisotropic diffusion (SRAD) filter (Yang and Clausi 2012; Choi and Jeong 2020a, b) is used for the despeckling of SAR images. This filter uses a window size of 9 × 9 that is a higher window size, and this is the drawback of the filter. The PCA-NLAM filter (Yousif and Ban 2013) uses a gamma MAP. The performance of the filter is slow, and it uses window sizes of 5 × 5 and 7 × 7. The drawback of this filter is high computational complexity. The Monte Carlo texture likelihood sampling (MCTLS) filter (Glaister et al. 2014) preserves the edges and structures. In this filter, the algorithm directly uses the noise distribution due to bias not reduced, and this is a drawback of the filter. This filter uses high window sizes of 7 × 7 and 11 × 11. SBGKF (Wu et al. 2014) preserves edges and lines, and it uses a ML rule. The drawback of this is that the kernel is not suitable for understanding the spatial relationship. The above filtering techniques are coming under spatial domain techniques. The ME-CT filter (Li et al. 2011) preserves high and low contrast edges. The reduction of speckle noise using this filter is poor. The BM3D-EWF filter (Parrilli et al. 2011) is efficient for speckle noise reduction because it eliminates the bias and it uses MMSE. This filter preserves the edge and texture regions. The drawback of this filter is while smoothing homogeneous areas, it shows relevant details. This filter uses lower window sizes of 1 × 1, 3 × 3, and 5 × 5. The wedge filter (Uslu and Albayrak 2013) is good for extracting the spatial features, and the drawback of this filter is robust against the speckle noise reduction. The patch order and transform domain filter (Xu et al. 2014) has the ability for speckle noise reduction, and it uses a lower window size of 3 × 3. The bias is removed using the patch order. But it preserves only structural information. The enhanced Lee filter (Hazarika et al. 2015) smooths the speckle noise well and retains more edges and textures. The wavelet shrinkage filter (Gao et al. 2016) directly affects the speckle reduction and details preservation performance. This is the drawback of the filter. The synthetic aperture radar block matching three dimensional (SAR-BM3D) filter (Di Martino et al. 2016) gives better edges and details by using visible artifacts in the homogeneous and flat regions. But this filter preserves only edges and textures. The above filtering techniques are coming under transform domain techniques. The CII-NLM filter (Xue et al. 2013) is good for the removal of speckle noise but it preserves only edges and shapes. The SDC filter (Yahya et al. 2014), an SDC function, is used as a size of the image and it uses a higher window size of 7 × 7 and this is the drawback of the filter. The MRF-NLM filter (Yousif and Ban 2014) preserves the details of geometric and spatial features, and it uses a higher window size of 7 × 7. The drawback of this filter is that the fine structures are removed. The above filtering techniques are coming under non-local filtering domain techniques. The FoE model is good for despeckling of SAR image, but it uses a higher window size of 7 × 7. The SDD filter (Ozcan et al. 2015) is preferred for homogenous regions, edges, and point scatterers. The homomorphic filter (Ma et al. 2016) uses to recover hyperspectral images that are affected by blurring. The above filtering techniques are coming under total variational techniques. From the investigation, it is understood that an image can be processed to full resolution of the azimuth and range resolution for each image cell in a single-look image. In the case of multi-look image processing, several neighboring image cells are integrated (averaged) usually in the azimuth direction since azimuth resolution is often several times better than range resolution. So multi-look image processing is more efficient than a single-look image. As the size of the window increases, smoothing also increases. So the amount of smoothing depends on the size of the window. When the size of the window is too large, there is a chance of blurring the important information in the image. The efficiency of despeckling is proportional to the window size.

The research gap is most of the speckle reduction techniques have been studied by researchers; however, there is no comprehensive method that takes all the constraints into consideration. Therefore, in this paper, we have performed a detailed study on the speckle reduction techniques and categorized it into various domains such as spatial, transform domain, non-local filtering, and variational techniques. The main contribution and novelty of the work is we have projected a detailed discussion on various classifications of speckle reduction filters and techniques used for suppressing the speckle noise. We have performed a detailed study on the reduction techniques and categorized it into various domains such as spatial, transform domain, non-local filtering, and variational techniques. We have compared the existing despeckling methods. This is done by determining the performance parameters. The analysis of speckle reduction filtering techniques is comparatively studied with varying filter window sizes and various database images.

Classification of speckle reduction filters

Speckle filtering will give better performance to recognize various target scenes and easy-to-do image segmentation. When selecting different analysis methods, the speckle noise is considered. An ideal speckle reduction filter can be used with a small amount of information loss. In the homogeneous areas, the filter can able to retain the edge and radiometric information. In the case of textured areas, the filter can preserve the texture information known as the variability of spatial signal and radiometric information. Figure 1 shows the classification of different filters.

The non-adaptive filters can be further classified based on mean and median. The intensity of the individual sample interval in the image is exchanged with the mean of the pixel values while moving the window around the sample. This is

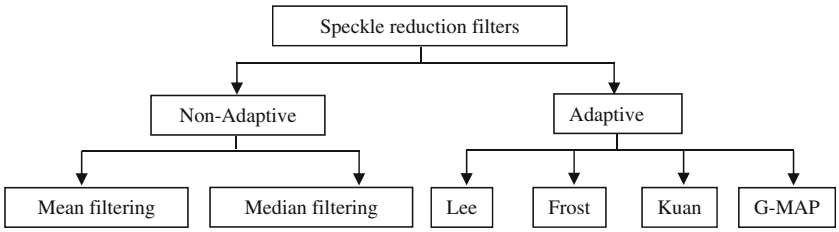

Fig. 1 Classification of speckle reduction filters

the basic principle used in non-adaptive filters. The advantage of a mean filter is that it can preserve the radiometry information but it blurs the texture area. This filter can preserve better texture information but it changes the homogeneous area (Wang et al. 2019). An example of a non-adaptive filter is the fast Fourier transform (FFT) filter. The adaptive filter performance is good compared with non-adaptive filters for minimizing the speckle noise. Adaptive filters have the advantage of considering the local characteristics of the terrain backscatter and it can also accommodate the local property changes. Some of the examples of adaptive filters are the Lee, Frost, Kuan, and MAP gamma filters.

The Lee filter can be used in the flat region to smooth away the noise leaving the high-quality information (text and lines) unchanged. It uses a small size of the window 3 × 3, 5 × 5, or 7 × 7. Using this window size, the local mean and variance are estimated. To retain the sharp details a region that maintains constant intensity and responds by smoothing, this Lee filter can be applied. The difficulty with this filter is it leaves the edge and line information. This filter can handle different variants like multiplicative noise and sharpening (Lee 1980). The Frost filter acts as an adaptive filter to suppress the speckle noise. This filter uses a negative exponential distribution and for the filtering process, this filter uses local image statistics. Using local image statistics, the Frost filter can give weights of each cell which is determined for various filter windows. The weight of a cell relies upon the distance calculation between the center cell and its neighboring cells. As the inside cells are intensely weighted due to changes in the filter window size variance, the Frost filter will smoothen the homogeneous areas. This can provide a close signal estimation to verify the detected range of the center cell in homogeneous areas. This filter does not have any user-defined parameters. The parameters are altered in each area concerning the variance. This is the drawback of the Frost filter. If the variance is low, then smoothing occurs. When the variance increases, only less smoothing happens and the edges are preserved (Frost et al. 1982). The Kuan filter is more useful than the Lee filter because it will not approximate the noise variance within the filter window. It simplifies by converting the multiplicative noise approach into an additive noise form. To perform the filtering process, this filter can depend on the estimated noise level of an image to define a weighting function (Kuan et al. 1985). In the gamma-maximum a posteriori (GMAP) filter, the speckle noise is assumed as the scene observation of an image as a Gaussian distribution. During speckle noise reduction in an image, this filter utilizes prior information of the probability distribution function (PDF) of the image. With non-stationary mean and variance parameters, the GMAP filter has been developed using a multiplicative noise approach. The mean and variance of the interested pixel and all pixels in the moving kernel are equal. This measured value is called a digital number (DN). The original DN values contain all of the information in the scene (Baraldi and Parmiggiani 1995).

Speckle noise reduction techniques

Generally, each visual representation of an image suffers from a problem of noise. Due to the unwanted data that can decrease the contrast, the shape or size of an object in an image can collapse and border edge blurring or changes in the image fine details can be called noise. Noise may appear due to the structure of the system, due to the illumination condition and mechanism used for acquiring an image. Speckle is a noise, which will decrease the clarity of the SAR images. Based on the mathematical model, Speckle is a multiplicative noise (D'Hondt et al. 2006). Multiplicative noise cannot be removed very easily because of the de-phased echoes from the appearing scatters. For suppression of speckle and despeckling in SAR images, various methods have been suggested over the last three decades. The important requirement of speckle reduction methods is that the speckle should be

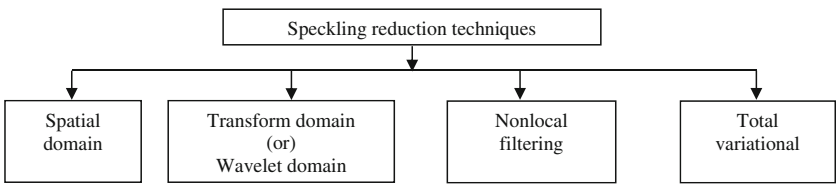

Fig. 2 Categories of speckling reduction techniques

Table 1 Comparison of various filtering techniques

Filter name	Preserved information	Technique	Features	Advantage	Limitations	Performance	Window size	Applications
Spatial domain techniques								
AGK-MMSE (D'Hondt et al. 2006)	Texture	Gradient structure tensor (GST)	Single-look	Texture preservation and structure enhancement	The bias is weak for homogeneous test areas	The quality of filtering is good	9 × 9	Classification
Mean shift (MS) (Jarabo-Amores et al. 2010)	Textures and edges	Agglomerative hierarchical clustering (AHC) Gaussian kernels	Multi-look	To map the coordinate system, there is no image rotation	Comparing the images with different resolutions is an issue	Filtering and segmentation results are quite good	3 × 3 5 × 5	Segmentation
SRAD filter (Yang and Clausi 2012; Choi and Jeong 2020a, b)	Edges	Instantaneous coefficient of variation (ICOV) is used to determine the strength of the edge	Multi-look	Speckle noise is appear while detecting the edges	Due to bias, the segmentation accuracy is affected	Due to the noise region level, Markov random field (MRF) model belongs to region-based representation	9 × 9	Segmentation
Principal component analysis (PCA)-non-local means (NLM) (Yousif and Ban 2013)	Preserves the shape of new objects	Gamma MAP	Not mentioned	Image fine structures	High computation complexity	Slow performance of the algorithm	5 × 5 7 × 7	Image restoration
MCTLS (Glaister et al. 2014)	Preserve edges and structures	Texture and Fisher tippett logarithmic space speckle distribution (SD) model	Multi-look	Models are rotationally invariant and take the spatial relationships within a texture	Bias is not reduced because the algorithm directly uses the noise distribution	Good despeckling	11 × 11 7 × 7	Segmentation and region classification
Sketch-based geometrical kernel function (SBGKF) (Wu et al. 2014)	Edges and lines	Maximal likelihood (ML) rule is used	Multi-look	To form a neighborwise similarity metric, a modified ratio distance is calculated	To understand spatial relationship, kernel is not suitable	Speckle looks are calculated	Not mentioned	Region growing
Empirical mode decomposition (EMD)–based filter (De la Mata-Moya et al. 2014)	Preserve edge information	Intrinsic mode functions (IMF)	Not mentioned	Basis functions are derived from the signal itself and hence, the analysis is adaptive	Not mentioned	Strongly depends on the type of clutter	3 × 3 5 × 5	Segmentation
Transform domain (or) wavelet domain techniques								
Mirror-extended curvelet transform (ME-CT) (Li et al. 2011)	High and low contrast edges	ME-CT with improved particle swarm optimization (IPSO)	Multi-look	Improve SAR image quality	Not effectively reducing the noise	Reduction of speckled noise is poor	Not mentioned	Feature enhancement of SAR images

Table 1 (continued)

Filter name	Preserved information	Technique	Features	Advantage	Limitations	Performance	Window size	Applications
BM3D-empirical Wiener filtering (EWF) (Parrilli et al. 2011)	Edge & textured regions	Local linear minimum mean squared error (LLMMSE)	Single-look	Bias is eliminated	Relevant details while smoothing homogeneous areas	Efficient speckle reduction	5 × 5 3 × 3 1 × 1	Segmentation and classification
Wedge filter (Uslu and Albayrak 2013)	Pixels along edges	Generalized Gaussian distribution (GGD) parameter estimation for curvelet subbands, content-based image retrieval (CBIR), histogram of curvelets (HoC)	Not mentioned	Inclusion of neighboring pixels for feature extraction	Robust against speckle noise	Good for extracting the spatial features	5 × 5	Classification
Patch ordering and transform domain filter (Xu et al. 2014)	Structural information	Simultaneous sparse coding (SSC)	Single-look	Using patch ordering bias is removed	Not mentioned	Good speckle reduction ability	3 × 3	Classification
Enhanced Lee filter (Hazarika et al. 2015)	Textures, edge	LOT, modified ratio of averages (MROA)	Single-look	Classifying edge and edge information retained during despeckling	Not mentioned	Smooths the speckle well and retains more edges and textures	Not mentioned	Classification
Wavelet shrinkage filter (Gao et al. 2016)	Edge information, image boundaries and textures	Two dimensional S-transform shrinkage (TDSTS) algorithm	Single-look	Possible to process large images	Does not always work well, particularly in more complex scenes	Directly affect the speckle reduction and detail preservation performance	Not mentioned	Segmentation and classification
SAR-BM3D filter (Di Martino et al. 2016)	Edges and textures	Small perturbation method (SPM) is used for natural surfaces. The sensed surface of the local incidence angle is determined using the digital elevation model (DEM)	Single-look	Improve prior information regarding the electromagnetic scattering of the detected surface	Not mentioned	It gives better edges and details by using visible artifacts in the homogeneous and flat regions	Not mentioned	Classification
Non-local filtering techniques								
Cosine integral images (CII)-NLM (Xue et al. 2013)	Edges and shapes	CII	Multi-look	CII method is used to speed up NLM filtering	Bias reduced	Speckle is well removed	Not mentioned	Edge detection
Spatial domain constraint (SDC) filter (Yahya et al. 2014)	Lines and edges	Subspace-based SDC approach	Single-look	Logarithmic transformation is used	Backscatter mean preservation in homogeneous areas, sharpness preservation	The SDC function is the size of the image	7 × 7	Remote sensing and monitoring applications
MRF-NLM (Yousif and Ban 2014)	Geometric details, spatial details	Iterated conditional modes (ICM) optimization	Not mentioned	Assigning the same class-labels to adjacent pixels and	Fine structures are removed	Noise level increases	7 × 7	Classification

Table 1 (continued)

Filter name	Preserved information	Technique	Features	Advantage	Limitations	Performance	Window size	Applications
				building homogeneously connected regions				
Total variational techniques								
Fields of experts (FoE) model (Chen et al. 2014)	The small structures in the image	Inertial proximal algorithm for non-convex optimization (iPiano)	Multi-look	Suitable for graphical processing unit (GPU) programming	Not mentioned	Good for despeckling	7 × 7	Classification
Sparsity-driven despeckling (SDD) filter (Ozcan et al. 2015)	Edges and point scatterers	Total variation (TV) approach	Not mentioned	Capable of using various norms controlled by a one parameter (f)	Not mentioned	Preferred for homogenous regions, edges, and point scatterers	Not mentioned	Edge detection and segmentation
Homomorphic filter (Ma et al. 2016)	The edges and boundaries between objects	Non-homomorphic adaptive non-local function (NHANLF) model	Single-look	Homomorphic transformation is often used as an additive model to change the multiplicative model	Combining with a structure tensor to recover hyperspectral images which are effected by blurring	NHANLF model attains better despeckling performance	3 × 3 7 × 7	Target detection and classification

minimized and the texture or edge information retained. The major speckle reduction techniques fall into four categories as shown in Fig. 2.

The spatial domain techniques have three difficulties. One is if the original SAR data is having a small number of looks, it fails to maintain the mean value. Second, it is difficult to see the highly reflective point objectives, and finally the dark spotted pixels are unfiltered. It is developed by using the MMSE criteria and MAP approaches (D'Hondt et al. 2006; Jarabo-Amores et al. 2010; Shui and Cheng 2012; Yang and Clausi 2012; Yousif and Ban 2013; Glaister et al. 2014; Zheng et al. 2014; Wu et al. 2014; De la Mata-Moya et al. 2014). The second category is the transform domain, based on the lapped orthogonal transform (LOT) domain and a logarithmic transformation. A logarithmic transformation is used to change the speckle noise in terms of additive noise (Moghimi et al. 2017). In the wavelet domain, filtering is performed by thresholding the wavelet coefficients of the noisy image (Li et al. 2011; Parrilli et al. 2011; Uslu and Albayrak 2013; Xu et al. 2014; Hazarika et al. 2015; Gao et al. 2016; Di Martino et al. 2016). The third category is non-local filtering, which is developed based on self-similarity measurement between the pixels (Sun et al. 2020). In non-local filtering, a summing method is used to estimate the image patch similarity with the help of mean values of image patches but it is independent of the kernel size (Xue et al. 2013; Yahya et al. 2014; Yousif and Ban 2014). The last category is variational techniques developed based on some appropriate energy functionals and consisting of a regularizer (also called image prior). Sometimes called total variation is the regularization of the total variation. It is a method used in digital image processing and has a noise reduction application. The basic principle is that the signals have unnecessary and probably false information with a full variation which is highly integral to the absolute gradient of the signal. Using this basic principle, the total variation of the signal due to it being close to the original signal is eliminated. So, while maintaining more important details such as edge information, it eliminates unwanted details (Woo and Yun 2011; Chen et al. 2014; Ozcan et al. 2015; Ma et al. 2016). Table 1 projects the comparative analysis of various filtering techniques in different categories with their performances and limitations. This table also discusses the preserved features of various filters applied to speckle noise images by various researchers. The advantages and limitations of various filters are also detailed along with the size of the images.

Results

In this paper, we have collected SAR images from Sandia National Laboratory. SAR images are related to Eubank Gate at Kirtland Air Force Base (the date of acquiring

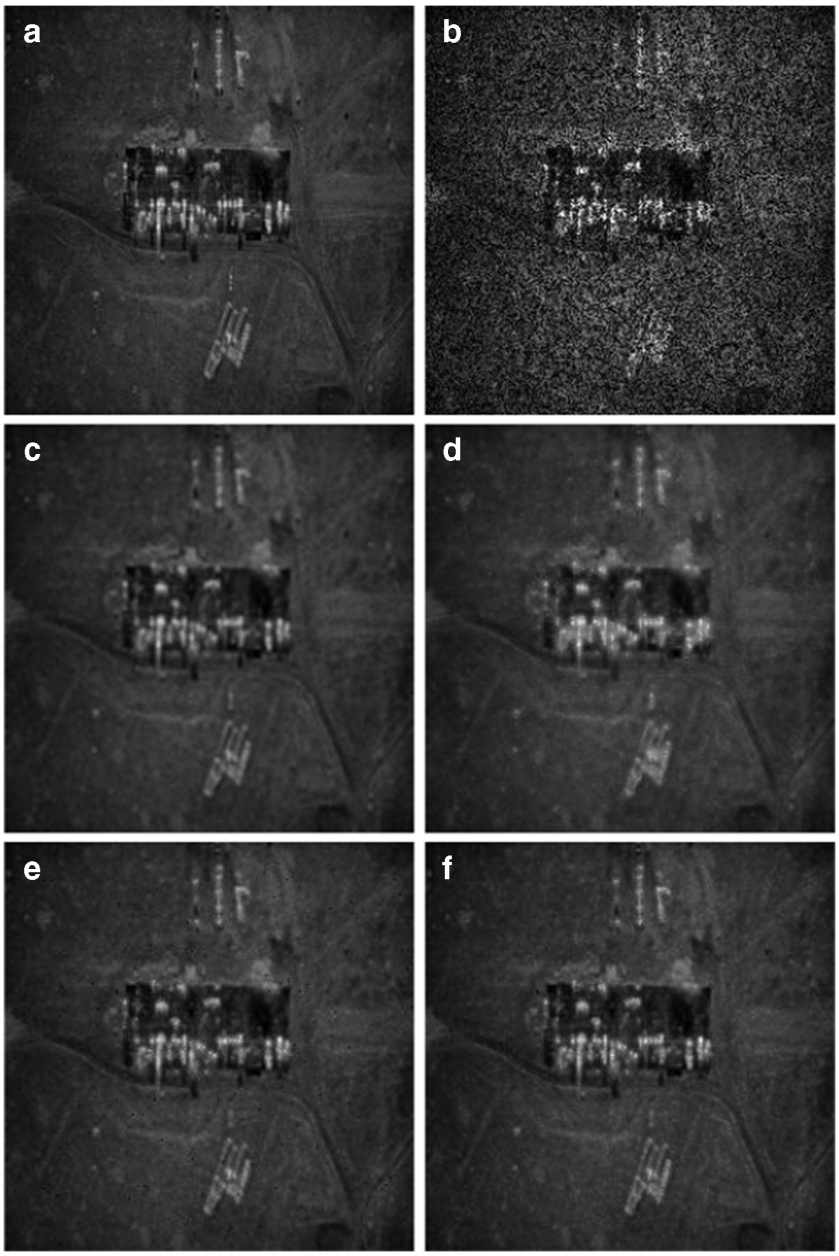

Fig. 3 SAR image with a variance of 0.05. **a** Database image. **b** SAR image with speckle noise. **c** Lee filter. **d** Kuan filter. **e** Frost filter. **f** GMAP filter

2006:03:01 and time of acquiring 14:31:01). We are using MATLAB R2020a software to carry out all simulation process. All the filters have been experimented in MATLAB on the system configuration of Intel Core i5-8050 CPU @3.2 GHz, 8 GB of RAM. Figure 3 shows the original SAR image, which is collected from the database. The noisy SAR image with a variance of 0.05 is shown in Fig. 3b. Now, Fig. 3b shows the input image to all the filters (Lee, Kuan, Frost, and GMAP filters). The despeckled SAR images for Lee, Kuan, Frost, and GMAP filters are shown in Fig. 3c, Fig. 3d, Fig. 3e, and Fig. 3f, respectively. Apart from all these filters, the GMAP filter will give better results. The SAR image with speckle noise of 0.04 is shown in Fig. 4a. Now, Fig. 4a is the input image to all the filters. The despeckled SAR images for Lee, Kuan, Frost, and GMAP filters are shown in Fig. 4b, Fig. 4c, Fig. 4d, and Fig. 4e, respectively. The variance of a speckled SAR image that is varied to 0.03 is shown in Fig. 5a. The despeckled SAR images for Lee, Kuan, Frost, and GMAP filters are shown in Fig. 5b, Fig. 5c, Fig. 5d, and Fig. 5e, respectively. The variance that is 0.02 of a speckle image is shown in Fig. 6a. The despeckled SAR images for Lee, Kuan, Frost, and GMAP filters are shown in Fig. 6b, Fig. 6c, Fig. 6d, and Fig. 6e, respectively.

From the visual representation of the despeckled images, it clearly shows the appearance is almost similar to the original image.

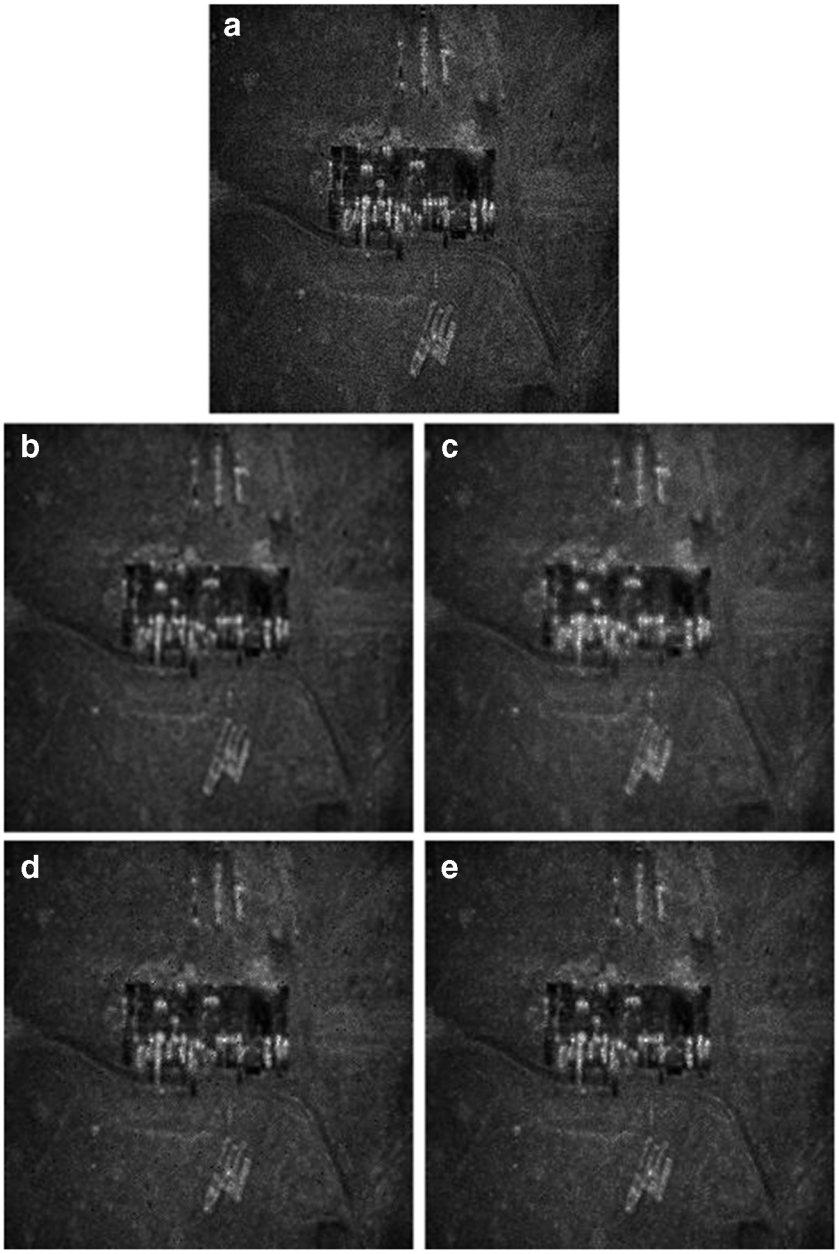

Fig. 4 SAR image with speckle noise of 0.04. **a** SAR image with speckle noise. **b** Lee filter. **c** Kuan filter. **d** Frost filter. **e** GMAP filter

Discussion

The performance of despeckling issues can be estimated using various parameters as shown in Table 2. The speckle level in a SAR image can be measured by using the ENL parameter. It gives information about how well the speckle noise is reduced without affecting the homogeneous areas.

This session provides an insight into the quantitative and qualitative values of the performance parameters listed in Table 2. The High values of parameters such as ENL, PSNR, EPI, CNR, and the Low values of SSI, SMPI are the good quality indices of the images after speckle reduction.

Figure 7 shows the theoretical and estimated ENL values on different homogeneous areas. Here, two filtering approaches, i.e., refined MMSE and AGK-MMSE, are discussed. The results are compared in terms of ENL values. The refined MMSE filter will blur the image pixels; thus, the quality of the image is degraded. This drawback can be overcome by using the AGK-MMSE filter as it could able to preserve the texture and structural details efficiently. The estimated ENL value shows AGK-MMSE filter can provide better performance. The filtered image using refined MMSE has an estimated ENL value of 15.8. A higher value of ENL improves the quality of the filter performance. The ENL parameter value depends on the size of the tested region. To analyze the result of different filters, the quantitative MSE parameter is also calculated. The SNR is not sufficient in the case of multiplicative noise for evaluating the noise reduction. If SNR is

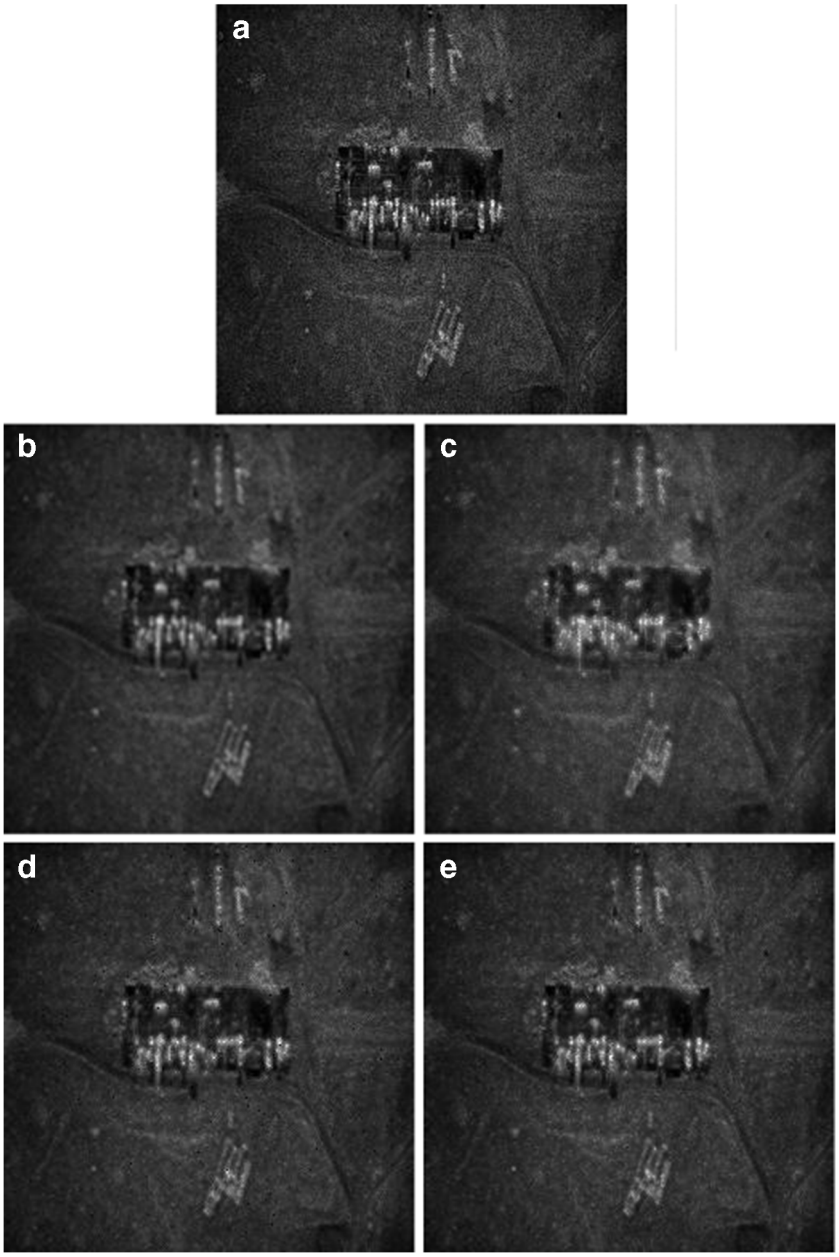

Fig. 5 Speckled SAR image that is varied to 0.03. **a** SAR image with speckle noise. **b** Lee filter. **c** Kuan filter. **d** Frost filter. **e** GMAP filter

measured in the case of additive noise, then it is called S/MSE. The filtered image using refined MMSE has an estimated ENL value of 15.8. In the case of the AGK-MMSE filter, the estimated ENL value is 17.9.

Figure 8 shows the S/MSE values for different images. By using a mean shift algorithm with Gaussian kernels, improved S/MSE values can be obtained. This figure shows a comparison of two different images. As the ENL value of an image increases, the S/MSE value also increases while applying mean shifting algorithm with Gaussian kernels. An S/MSE value of 12.38 and 15.71 has been obtained for ENL = 1 and 2 with Gaussian kernels $h_s = 2$ and $h_r = 1$. This algorithm is also tested on a Lena image with the same ENL, and the S/MSE values of 8.98 and 10.87 are obtained.

Figure 9 shows the ENL values using different filters in SAR images. The quality of the despeckled image is also measured with the help of the PSNR parameter. If the PSNR value is higher, it shows a better quality of an image. A comparative analysis of ENL values with PSNR has been performed and plotted in Fig. 9. We have analyzed the performance of both adaptive and non-adaptive filters in terms of ENL under different scenes. Scenes are the selected regions of the image based on pixel intensities. Even though the adaptive filters such as the Lee filter, gamma MAP filter, and Frost filter give better performance in terms of ENL values and appear smooth, it results in a blurred image. By applying the SRAD algorithm, the edge information can be retained and the scene appearance is too smooth in the homogeneous region

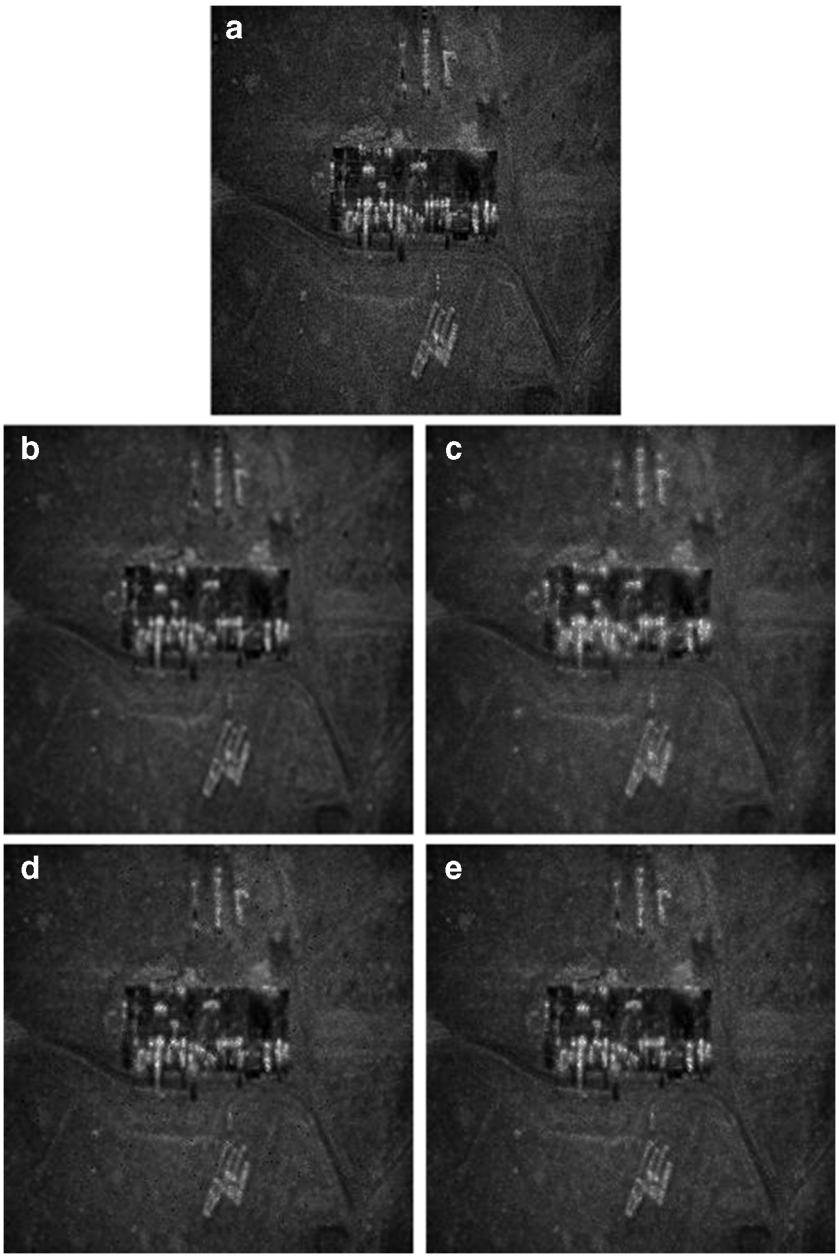

Fig. 6 Variance that is 0.02 of a speckle image. **a** SAR image with speckle noise. **b** Lee filter. **c** Kuan filter. **d** Frost filter. **e** GMAP filter

Table 2 Performance of different parameters

Parameters	Performance
Equivalent number of looks (ENL)	Higher
Signal to mean squared error (S/MSE)	Higher
Peak signal to noise ratio (PSNR)	Higher
Speckle suppression index (SSI)	Lower
Speckle suppression and mean preservation index (SMPI)	Lower
Edge preservation index (EPI) or edge save index (ESI)	Higher
Contrast to noise ratio (CNR)	Higher
Structural similarity (SSIM)	Between 1 and − 1
Figure of merit (FOM)	Between 0 to 1

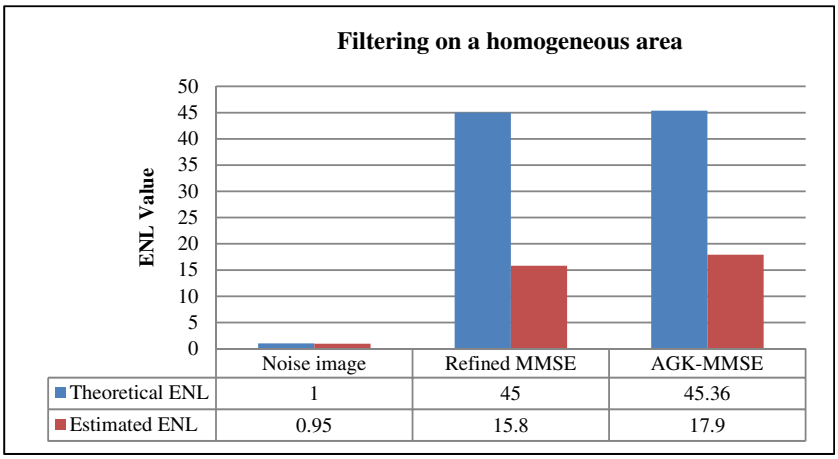

Fig. 7 Comparison of theoretical and estimated ENL

(Choi and Jeong 2020a, b). Therefore, bilateral wavelet-based filtering is used to reduce noise, but it suffers from a lack of accurate image coefficients (Ai et al. 2019). Regarding speckle noise reduction, the block matching three dimensional (BM3D) and MCTLS algorithms work comparably. For all three SAR scenes, the MCTLS algorithm has a lower ENL than BM3D. If ENL value is higher for an image, it provides more efficient noise reduction in the homogeneous areas (Glaister et al. 2014).

Figure 10 illustrates the PSNR values obtained for various images using SAR-BM3D and homomorphic block matching three dimensional (H-BM3D) algorithms. The SAR-BM3D method is developed based on wavelet-domain shrinkage and non-local filtering. This method can be enhanced with the block matching 3D (BM3D) algorithm. This algorithm can be used in two different stages. The first stage is the block matching stage that is used to measure probabilistic similarity. The second stage is the wavelet shrinkage stage, which develops an additive signal-dependent model. The following method H-BM3D deals with images having a large number of looks. H-BM3D provides an acceptable balance between smoothing and detail preservation. As minimal ENL values are considered in SAR-BM3D, the edge information is lost and we get less PSNR values. These images are tested using this algorithm and a PSNR value of approximately 25 is achieved with ENL values of 1 and 2. The higher values of ENL as ENL = 4 and ENL = 6 are considered in the H-BM3D algorithm. Here, a PSNR value of about 35 is attained, and this shows that the edge details are preserved than SAR-BM3D (Parrilli et al. 2011).

Apart from these parameters, few more parameters can also be used to analyze the performance and gather more information. Here, we discuss some of the parameters which can evaluate the SAR image. The SSI parameter is used to indicate the quantity of speckle suppressed. If the SSI parameter value is less, then more quantity of speckle noise is suppressed. When the filter is overestimated, the mean ENL value and SSI parameters are not sufficient for measuring the quality of speckle reduction. So the SMPI parameter is used to measure the amount of speckle suppression. EPI or ESI is used to analyze the edge preservation capability. CNR is used to compute the image quality. To determine the matching of two images, the SSIM parameter is used. This parameter value is between 1 and − 1. For better restoration, it requires higher SSIM values. The FOM is used to evaluate the edge preservation of various speckle reduction techniques. The FOM value is between 0 and 1. Table 3

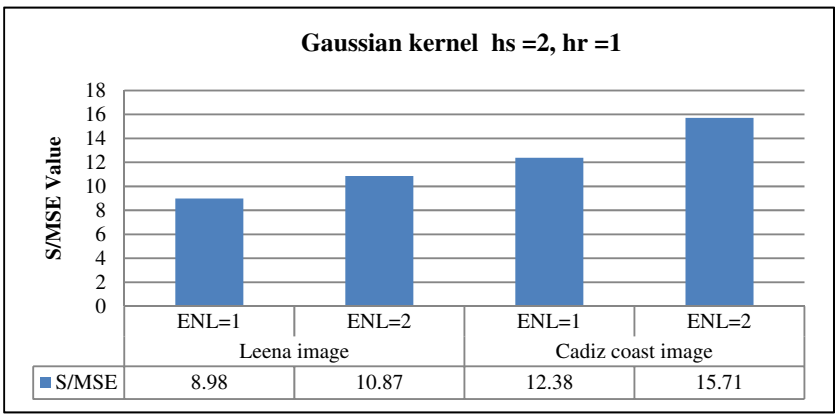

Fig. 8 ENL vs S/MSE with Gaussian kernel

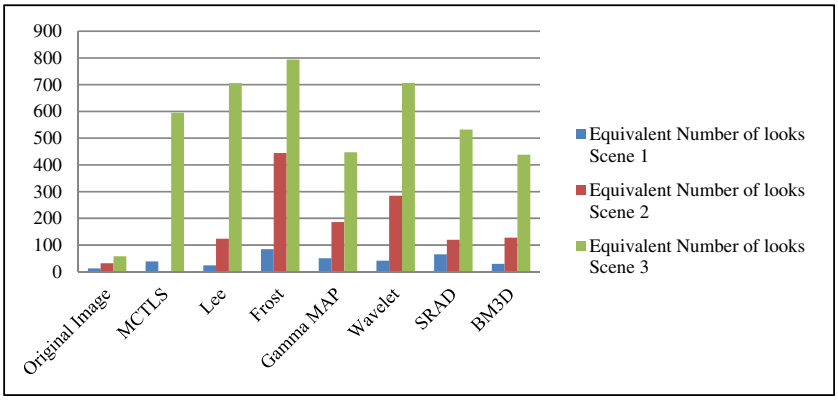

Fig. 9 ENL for different SAR scenes

summarizes the different filtering methods along with the image database and size used for testing. A good despeckling technique can be validated based on window size, various performance parameters, image size, and multi-look image. There is always a tradeoff between speckle reduction and detail preservation.

Conclusion

This paper has projected a detailed discussion on various classifications of speckle reduction filters and techniques used for suppressing the speckle noise. In SAR image processing, two important issues are considered: one is speckle reduction and the other is detail preservation. To increase the performance of noise reduction methods, it is necessary to introduce the concept of multiresolution analysis. In the direction of SAR satellite imaging technology, speckle noise reduction seems to be one of the most promising applications. Different applications may require different balances between speckle reduction and detail preservation. We have performed a detailed study on the speckle reduction techniques and categorized it into various domains such as spatial, transform domain, non-local filtering, and variational techniques. The quantitative analysis of different filtering methods makes us conclude that a good despeckling technique can be validated based on window size, image size, and multi-look, and by various performance indices.

Future challenges and possible solutions

We have explored a vast review of popular filters applicable to speckle noise minimization. The filtering process is continued from the perspective of preserving the original information and removing unwanted speckle components. The selection of best filtering approaches for an SAR image is still not optimized and we have to uncover more methodology. This analysis can be explored in two domains, such as spatial and transform domain. To increase the performance of the despeckling algorithms, the analysis of multiresolution has been discovered in the past two decades. The essential key features of wavelet-based speckle reduction using the reflectivity of the modeling and in the wavelet domain of the signal-dependent noise and to obtain the noise-free wavelet coefficients, the selection of the estimation model is used. Few authors have preferred the overfitting models, while few others have decided to maintain their space and scale adaptivity. This is done by using pdfs and using some parameters that are determined locally on subbands/frames. Speckle noise reduction is a pre-processing step that must preserve the radiometry information of an image and a segmented model. The sample statistics are contained on uniform segments by using

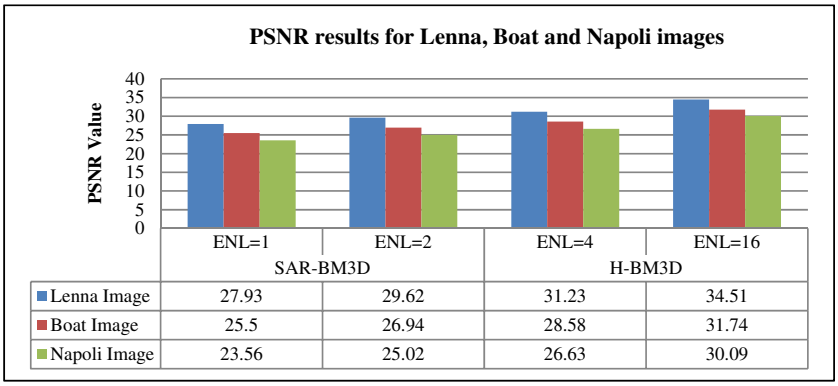

Fig. 10 Number of looks vs PSNR with different images

Table 3 Summary of filter methods with database images

Methods	Database used for testing	Image size
AGK-MMSE (D'Hondt et al. 2006)	Weiherbachtal data set (ESAR, DLR)	1024 × 1024, 416 × 235
MS-GK (Jarabo-Amores et al. 2010)	Lena image, Galicia coast, Jutland's west coast, Google Earth's Cadiz (Spain) coastal image	Not mentioned
GGS bi-windows (Shui and Cheng 2012)	Synthetic cartoon image	512 × 512
SRAD filter (Yang and Clausi 2012; Choi and Jeong 2020a, b)	SAR sea ice images captured by RADARSAT-2 in Quad-Polarization mode over Liaodong Bay, China, on January 14, 2009, SAR image captured over the Gulf of Saint Lawrence	Not mentioned
PCA-NLM (Yousif and Ban 2013)	Beijing: ERS-2 27/09/1998, ERS-2 07/09/1999 Shanghai: ENVISAT-23/09/2008, ENVISAT-19/09/2008	666 × 718
MCTLS (Glaister et al. 2014)	Three SAR scenes (MacDonald, Dettwiler and Associates Ltd. 2010)	512 × 512
PPB FILLTER (Zheng et al. 2014)	Bern data set : Image acquired in April 1999, image acquired in May 1999 Ottawa data set: Image acquired in July 1997, image acquired in August 1997 Yellow River data set A and B: Image taken in 2008, image taken in 2009	301 × 301 290 × 350
SBGKF (Wu et al. 2014)	SAR images of different Malaysian terrains: Kota Bharu, Perlis, Sibu, Lembah Klang (Malaysian Remote Sensing Agency's courtesy)	256 × 256, 300 × 300, 390 × 500
EMD-based filter (De la Mata-Moya et al. 2014)	Land area, sea area	52,400 × 37,200
ME-CT (Li et al. 2011)	Horse track, Stanwick, Noerdlingen, Volgograd	Not mentioned
BM3D (Parrilli et al. 2011)	Lena, Boat, Napoli, SAR-X images (Infoterra GmbH)	512 × 512, 256 × 256
Patch ordering and transform domain filter (Xu et al. 2014)	Peppers, Cameraman, Dalian, and Flevoland	256 × 256 600 × 600
Enhanced Lee filter (Hazarika et al. 2015)	Horse track and Stadium	30 × 43, 40 × 35, 25 × 43, 37 × 21
Wavelet shrinkage filter (Gao et al. 2016)	Three scenes of real SAR images	500 × 500, 768 × 538
SAR-BM3D filter (Di Martino et al. 2016)	COSMO-SkyMed single-look strip map SAR volcano image near Naples, Italy.	512 × 512, 1700 × 1200, 1000 × 1000
CII-NLM (Xue et al. 2013)	Lena, Boat, Real SAR image	256 × 256, 512 × 512, 1024 × 1024
SDC filter (Yahya et al. 2014)	Real SAR image (estuary near Yellow River in China, C-band, 8-m resolution, four-look), Filed, Town, Horse Track	8930 × 8851, 8934 × 8845, 8148 × 6963, 8966 × 8926, 7090 × 7660
MRF-NLM (Yousif and Ban 2014)	Images from Beijing: ERS-SAR 19 July 1998; ENVISAT ASAR 15 July 2008 Images from Shanghai: ERS-SAR 29 June 1999; ENVISAT ASAR 20 July 2009	600 × 600, 999 × 883, 666 × 718
PPB (Woo and Yun 2011)	Barbara, Boat, House, Lena, eight remote sensing images & 2 real SAR images	256 × 256 to 1500 × 1500
FoE Model (Chen et al. 2014)	Lena, Peppers, and Couple	256 × 256, 512 × 512, 481 × 321
SDD filter (Ozcan et al. 2015)	Lena, TerraSAR-X spotlight with urban areas, TerraSAR-X spotlight with forest areas, TerraSAR-X StripMap and Sentinel with land and sea	1024 × 1024, 2048 × 2048, 4096 × 4096, 8192 × 8192
Homomorphic filter (Ma et al. 2016)	Oberpfaffenhofen image, Flevoland image	10,000 × 100,000, 1540 × 2816

the wavelet domain Bayesian despeckling techniques. To build hybrid filters, the fuzzy filters are combined with classical filters. The main shortcoming of the fuzzy-based filters compared to the classical filters is its inability to deal with images that are affected by noise. Applying fuzzy filters makes it possible to extract the details about the neighborhood pixels even from degraded images.

Given the enormous work of researchers in this area, the latest developments and applications to speckle noise reduction techniques are expected in the future. The major drawback of the compressed sensing-based algorithms and wavelet domain Bayesian-based algorithms is the computational issue. The multiprocessor models will be more applicable for efficiently correlated methods. In the future, this area of research

is to develop efficient and better despeckling methods for SAR images. The complexity of traditional filters can be overcome with the help of suitable algorithms. This will be useful for increasing the filter performance. To increase the quality of the image, different new performance parameters can be generated and used for the analysis of denoising filters.

References

Ahmed AA, Pradhan B, Sameen MI, Makky AM (2018) An optimized object-based analysis for vegetation mapping using integration of Quickbird and Sentinel-1 data. Arab J Geosci 11:280. https://doi.org/10.1007/s12517-018-3632-1

Ai J, Liu R, Tang B, Jia L, Zhao J, Zhou F (2019) A refined bilateral filtering algorithm based on adaptively-trimmed-statistics for speckle reduction in SAR imagery. IEEE Access 7:103443–103455. https://doi.org/10.1109/ACCESS.2019.2931572

Baraldi A, Parmiggiani F (1995) A refined gamma MAP SAR speckle filter with improved geometrical adaptivity. IEEE Trans Geosci Remote Sens 33(5):1245–1257. https://doi.org/10.1109/36.469489

Chen Y, Feng W, Ranftl R, Qiao H, Pock T (2014) A higher-order MRF based variational model for multiplicative noise reduction. IEEE Signal Process Lett 21(11):1370–1374. https://doi.org/10.1109/LSP.2014.2337274

Choi H, Jeong J (2020a) Speckle noise reduction technique for SAR images using SRAD and gradient domain guided image filtering. In International Workshop on Advanced Imaging Technology (IWAIT) International Society for Optics and Photonics 11515: 115152 M. https://doi.org/10.1117/12.2566244

Choi H, Jeong J (2020b) Despeckling algorithm for reducing speckle noise in images generated from active sensors. Electron Lett 56(17):876–879. https://doi.org/10.1049/el.2020.0614

D'Hondt O, Ferro-Famil L, Pottier E (2006) Nonstationary spatial texture estimation applied to adaptive speckle reduction of SAR data. IEEE Geosci Remote Sens Lett 3(4):476–480. https://doi.org/10.1109/LGRS.2006.876223

Das AJ, Talukdar AK, Sarma KK (2013) An adaptive SAR image despeckling algorithm using stationary wavelet transform. Int J Electron Signals Syst (IJESS) 3(1):56–61

De la Mata-Moya D, Diaz-Soria A, Martin-de-Nicolas J, Jarabo-Amores MP, Pelaez, VM (2014) Spatially adaptive thresholding of the empirical mode decomposition for speckle reduction purposes. In EUSAR 10th European Conference on Synthetic Aperture Radar 1-4

Di Martino G, Di Simone A, Iodice A, Poggi G, Riccio D, Verdoliva L (2016) Scattering-based SARBM3D. IEEE J Sel Top Appl Earth Observ Remote Sens 9(6):2131–2144. https://doi.org/10.1109/JSTARS.2016.2543303

Ezzine A, Darragi F, Rajhi H, Ghatassi A (2018) Evaluation of Sentinel-1 data for flood mapping in the upstream of Sidi Salem dam (Northern Tunisia). Arab J Geosci 11:170. https://doi.org/10.1007/s12517-018-3505-7

Frost VS, Stiles JA, Shanmugan KS, Holtzman JC (1982) A model for radar images and its application to adaptive digital filtering of multiplicative noise. IEEE Trans Pattern Anal Mach Intell 2:157–166. https://doi.org/10.1109/TPAMI.1982.4767223

Gao F, Xue X, Sun J, Wang J, Zhang Y (2016) A SAR image despeckling method based on two-dimensional S transform shrinkage. IEEE Trans Geosci Remote Sens 54(5):3025–3034. https://doi.org/10.1109/TGRS.2015.2510161

Glaister J, Wong A, Clausi DA (2014) Despeckling of synthetic aperture radar images using Monte Carlo texture likelihood sampling. IEEE Trans Geosci Remote Sens 52(2):1238–1248. https://doi.org/10.1109/TGRS.2013.2248739

Gromek A, Castaldo L (2013) Collaborative filtering technique for SAR image speckle noise suppression. IEEE Signal Process Symp (SPS): 1–4. https://doi.org/10.1109/SPS.2013.6623570

Haldar D, Rana P, Hooda RS (2019) Biophysical parameter assessment of winter crops using polarimetric variables—entropy (H), anisotropy (A), and alpha (α). Arab J Geosci 12:375. https://doi.org/10.1007/s12517-019-4516-8

Hazarika D, Nath VK, Bhuyan M (2015) A lapped transform domain enhanced Lee filter with edge detection for speckle noise reduction in SAR images. IEEE 2nd Int Conf Recent Trends Inform Syst (ReTIS):243–248. https://doi.org/10.1109/ReTIS.2015.7232885

Jarabo-Amores P, Rosa-Zurera M, de la Mata-Moya D, Vicen-Bueno R, Maldonado-Bascon S (2010) Spatial-range mean-shift filtering and segmentation applied to SAR images. IEEE Trans Instrum Meas 60(2):584–597. https://doi.org/10.1109/TIM.2010.2052478

Kuan DT, Sawchuk AA, Strand TC, Chavel P (1985) Adaptive noise smoothing filter for images with signal-dependent noise. IEEE Trans Pattern Anal Mach Intell 2:165–177. https://doi.org/10.1109/TPAMI.1985.4767641

Lee JS (1980) Digital image enhancement and noise filtering by use of local statistics. IEEE Trans Pattern Analy Mach Intell 2:165–168. https://doi.org/10.1109/TPAMI.1980.4766994

Li Y, Gong H, Feng D, Zhang Y (2011) An adaptive method of speckle reduction and feature enhancement for SAR images based on curvelet transform and particle swarm optimization. IEEE Trans Geosci Remote Sen 49(8):3105–3116. https://doi.org/10.1109/TGRS.2011.2121072

Ma X, Shen H, Zhao X, Zhang L (2016) SAR image despeckling by the use of variational methods with adaptive nonlocal functionals. IEEE Trans Geosci Remote Sens 54(6):3421–3435. https://doi.org/10.1109/TGRS.2016.2517627

Mansourpour M, Rajabi MA, Blais, JAR (2006) Effects and performance of speckle noise reduction filters on active radar and SAR images. In Proc. ISPRS 36(1):W41

Mi H, Qiao G, Wang W, Hong Y (2019) Analysis of urban growth from 1960 to 2015 using historical DISP and Landsat time series data in Shanghai. Arab J Geosci 12:250. https://doi.org/10.1007/s12517-019-4420-2

Moghimi A, Khazai S, Mohammadzadeh A (2017) An improved fast level set method initialized with a combination of k-means clustering and Otsu thresholding for unsupervised change detection from SAR images. Arab J Geosci 10:293. https://doi.org/10.1007/s12517-017-3072-3

Murugesan K, Balasubramani P, Murugan PR (2020) A quantitative assessment of speckle noise reduction in SAR images using TLFFBP neural network. Arab J Geosci 13:35. https://doi.org/10.1007/s12517-019-4900-4

Oikonomidis D, Pavlides S (2017) Geological mapping of Santorini Volcanic Island (Greece), with the combined use of Pleiades 1A and ENVISAT satellite images. Arab J Geosci 10:175. https://doi.org/10.1007/s12517-017-2972-6

Ozcan C, Sen B, Nar F (2015) Sparsity-driven despeckling for SAR images. IEEE Geosci Remote Sens Lett 13(1):115–119. https://doi.org/10.1109/LGRS.2015.2499445

Parrilli S, Poderico M, Angelino CV, Verdoliva L (2011) A nonlocal SAR image denoising algorithm based on LLMMSE wavelet shrinkage. IEEE Trans Geosci Remote Sens 50(2):606–616. https://doi.org/10.1109/TGRS.2011.2161586

Rajamani A, Krishnaveni V (2014) Performance analysis survey of various SAR image despeckling techniques. Int J Comput Appl 90(7). https://doi.org/10.5120/15584-4254

Shui PL, Cheng D (2012) Edge detector of SAR images using Gaussian-gamma-shaped bi-windows. IEEE Geosci Remote Sens Lett 9(5): 846–850. https://doi.org/10.1109/LGRS.2012.2184521

Sun ZP, Liu S, Cao F, Shi Y, Wang CZ (2017) Fine classification of construction land using high-resolution remote sensing images: a case study in planning restricted zone of nuclear power plant. Arab J Geosci 10:495. https://doi.org/10.1007/s12517-017-3248-x

Sun Y, Lei L, Guan D, Li X, Kuang G (2020) SAR image change detection based on nonlocal low-rank model and two-level clustering. IEEE J Sel Top Appl Earth Observ and Remote Sens 13:293–306. https://doi.org/10.1109/JSTARS.2019.2960518

Uslu E, Albayrak S (2013) Curvelet-based synthetic aperture radar image classification. IEEE Geosci Remote Sens Lett 11(6):1071–1075. https://doi.org/10.1109/LGRS.2013.2286089

Wang Y, Li CH, Hou ZQ (2019) Mechanical behaviors of bimsoils during triaxial deformation revealed using real-time ultrasonic detection and post-test CT image analysis. Arab J Geosci 12:10. https://doi.org/10.1007/s12517-018-4179-x

Woo H, Yun S (2011) Alternating minimization algorithm for speckle reduction with a shifting technique. IEEE Trans Image Process 21(4):1701–1714. https://doi.org/10.1109/TIP.2011.2176345

Wu J, Liu F, Jiao L, Zhang X, Hao H, Wang S (2014) Local maximal homogeneous region search for SAR speckle reduction with sketch-based geometrical kernel function. IEEE Trans Geosci Remote Sens 52(9):5751–5764. https://doi.org/10.1109/TGRS.2013.2292081

Xu B, Cui Y, Li Z, Zuo B, Yang J, Song J (2014) Patch ordering-based SAR image despeckling via transform-domain filtering. IEEE J Sel Top Appl Earth Observ Remote Sens 8(4):1682–1695. https://doi.org/10.1109/JSTARS.2014.2375359

Xue B, Huang Y, Yang J, Shi L, Zhan Y, Cao X (2013) Fast nonlocal remote sensing image denoising using cosine integral images. IEEE Geosci Remote Sens Lett 10(6):1309–1313. https://doi.org/10.1109/LGRS.2013.2238603

Yahya N, Kamel NS, Malik AS (2014) Subspace-based technique for speckle noise reduction in SAR images. IEEE Trans Geosci Remote Sens 52(10):6257–6271. https://doi.org/10.1109/TGRS.2013.2295824

Yang X, Clausi DA (2012) Evaluating SAR sea ice image segmentation using edge-preserving region-based MRFs. IEEE J Sel Top App Earth Observ Remote Sens 5(5):1383–1393. https://doi.org/10.1109/JSTARS.2012.2217940

Yousif O, Ban Y (2013) Improving urban change detection from multitemporal SAR images using PCA-NLM. IEEE Trans Geosci Remote Sens 51(4):2032–2041. https://doi.org/10.1109/TGRS.2013.2245900

Yousif O, Ban Y (2014) Improving SAR-based urban change detection by combining MAP-MRF classifier and nonlocal means similarity weights. IEEE J Sel Top Appl Earth Observ and Remote Sens 7(10): 4288–4300. https://doi.org/10.1109/JSTARS.2014.2347171

Zheng Y, Zhang X, Hou B, Liu G (2014) Using combined difference image and k-means clustering for SAR image change detection. IEEE Geosci Remote Sens Lett 11(3):691–695. https://doi.org/10.1109/LGRS.2013.2275738